IOP Conference Series: Earth and Environmental Science

PAPER • OPEN ACCESS

Characteristics of zinc ferrite nanoparticles ($ZnFe_2O_4$) from natural iron ore

To cite this article: S Husain *et al* 2021 *IOP Conf. Ser.: Earth Environ. Sci.* **758** 012001

IOP Conf. Series: Earth and Environmental Science **758** (2021) 012001 doi:10.1088/1755-1315/758/1/012001

Characteristics of zinc ferrite nanoparticles ($ZnFe_2O_4$) from natural iron ore

S Husain[1*], M Yusup[1], N H Haryanti[1], Suryajaya[1], M Saukani[2], Rodiansono[3], S Arjo[4], A Riyanto[5]

[1] Department of Physics, Lambung Mangkurat University, Jl. A. Yani KM. 36 Banjarbaru, South Kalimantan, Indonesia
[2] Department of Mechanical Engineering, Islamic University of Kalimantan MAB, Jl. Adhyaksa No 2 Kayu Tangi Banjarmasin, 70123 Indonesia
[3] Department of Chemistry, Lambung Mangkurat University, Jl. A. Yani KM. 36 Banjarbaru, South Kalimantan, Indonesia
[4] Department of Physics Education, Prof. Muhammadiyah University Dr. Hamka Jakarta, Indonesia
[5] Department of Physics, Lampung University, Indonesia

Corresponding Author: sadanghusain@ulm.ac.id

Abstract. Synthesis of zinc ferrite nanoparticles ($ZnFe_2O_4$) of iron ore taken in Tanah Laut has been done. The Synthesis uses the coprecipitation method. $ZnFe_2O_4$ nanoparticles were characterized using X-Ray Diffraction (XRD), Transmission Electron Microscopy (TEM), Vibrating Sample Magnetometer (VSM), Fourier Transform Infrared (FTIR), and UV-Vis Spectrophotometer. Using XRD, it was found that $ZnFe_2O_4$ has an average crystal size of 8.80 nm. $ZnFe_2O_4$ is superparamagnetic because it has a narrow loop area of about 10 kOe.emu/g. Using FTIR, the Zn-O and Fe-O groups were obtained at wave numbers 556.58 and 598.87 cm^{-1}. The absorption spectrum is in the range of UV light (200 nm) to visible light (600 nm) and at wavelength of 288 nm is observed absorption.

1. Introduction

Zinc ferrite ($ZnFe_2O_4$) Nanoparticles are one of the most developed materials because they can be used in many applications including hyperthermia therapy, biomolecular sensors, and drug delivery [1]. $ZnFe_2O_4$ nanoparticles also have the potential to be applied as cancer therapy [2], gas sensors [3], photocatalysts [4], MRI [5], and other potentials. $ZnFe_2O_4$ nanoparticles have potential to be applied in the medical field because they have superparamagnetic properties at room temperature [5]. The magnetization of the $ZnFe_2O_4$ nanoparticles increased with decreasing particle size [6].

Research on $ZnFe_2O_4$ has been conducted by several researchers, such as that conducted by Asmin et al (2015) using the coprecipitation method and stated that the higher the magnetization value the smaller the α-Fe_2O_3 phase ratio with a maximum magnetization value of 16.510 emu/g at 15 kOe [6]. Nurhasanah and Richardina (2018) using the precipitation method for the synthesis of $ZnFe_2O_4$ concluded that the formation of the ferrite cubic spinel structure was observed in the X-ray diffraction pattern (XRD) and the spectrum Fourier Transform Infrared (FTIR) [7]. Spinel ferrite can be obtained by coprecipitation method using zinc chloride and ferric chloride as raw materials [8]. The results show that $ZnFe_2O_4$ is formed when the molar ratio of Zn/Fe is 1: 2 at pH = 7.5. Olmos et al (2016) used a method mechanochemical, stating that $ZnFe_2O_4$ exhibits superparamagnetic behavior at room temperature [9]. Vinosha et al (2017) using the coprecipitation method, the results obtained by the Vibrating Sample Magnetometer (VSM) from ZnFe2O4 are ferromagnetic [10].

This research is focused on $ZnFe_2O_4$ nanoparticles from natural iron ore. We predict natural iron ore can be used as raw material for $ZnFe_2O_4$ nanoparticles. Previous research successfully produced Fe_3O_4 nanoparticles [11,12]. Many Researchers use commercial materials to synthesize $ZnFe_2O_4$ [3,10,13-17]. This paper shows some characteristics $ZnFe_2O_4$ from natural iron ore such as magnetic properties, structure, and optic characteristic.

2. Materials and Methods

The Materials used were iron ore, 12 M HCl (aldrich), $FeSO_4.7H_2O$ (aldrich) 0.2M, NH_4OH (aldrich) 5%, $ZnCl_2$ 0.1M (aldrich), distilled water, aquabides, 96% ethanol. Mortar, 230 mesh sieve, Hot plate, Magnetic Stirrer bar, Oven, XRD, TEM, VSM 250, FTIR, and spectrophotometer UV-VIS. The material used in this study is iron ore taken from Tanah Laut Regency, South Kalimantan. Iron ore is obtained from boulders containing iron (Fe) in the form of iron oxide minerals, namely Magnetite (Fe_3O_4), Maghemite (γ- Fe_2O_3), and Hematite (α- Fe_2O_3) [11] and the rest are elements others such as Si, Cr, Mn, Ca, Br, La and Cu [18]. The research flow is shown in Figure 1.

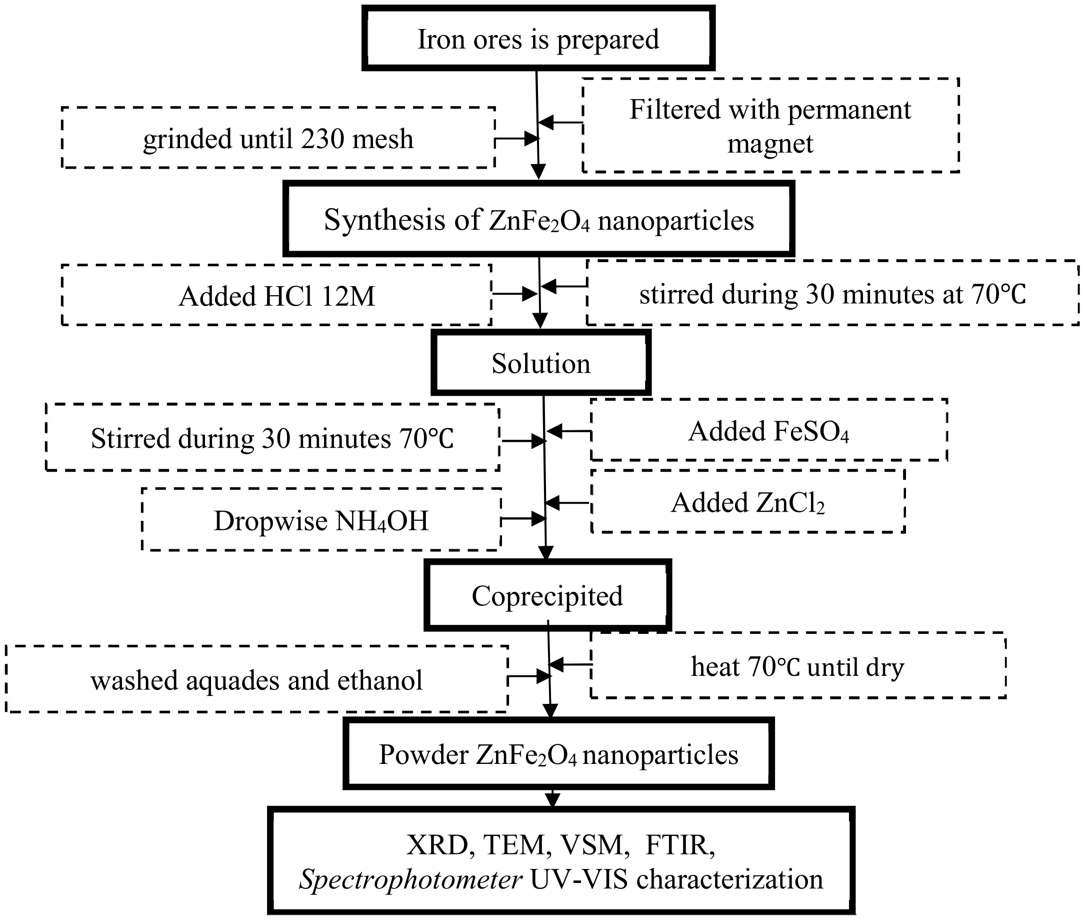

Figure 1. Research flowchart.

The synthesis process of $ZnFe_2O_4$ was done by the coprecipitation method as has been done previously with modification [12]. The cleaned iron ore is ground to form a powder to pass a 230 mesh sieve (Figure 2(a)). The powder is purified using a permanent magnet. 6 g of iron ore is dissolved by adding HCl to form a yellow solution (Figure 2(b)). To the solution, $FeSO_4$ 0.2M was added 0.4 g. The

IOP Conf. Series: Earth and Environmental Science **758** (2021) 012001 doi:10.1088/1755-1315/758/1/012001

solution is heated on a hot plate at a temperature of 70ºC and time is 15 minutes. Then, the solution was added $ZnCl_2$ 0.1M 0.2 g. The solution was dropped NH_4OH 5% until a thick black solution (Figure 2(c)). The sample was washed using distilled water three times and ended using 96% ethanol, then ultrasonicated. Samples were dried at 70ºC. powdered samples were characterized using XRD, TEM, VSM, FTIR and UV-Vis.

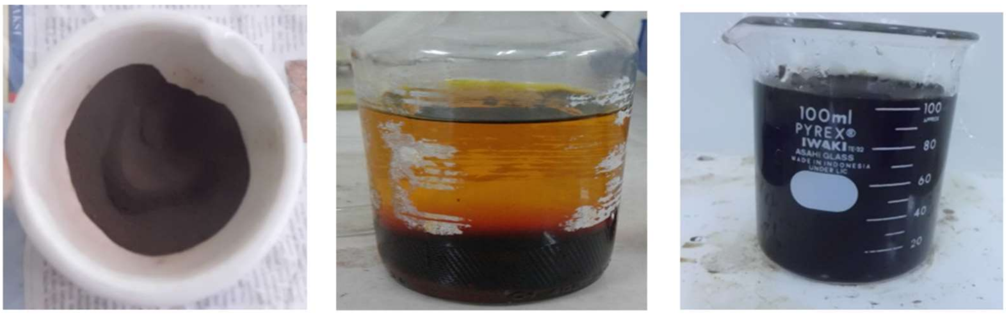

Figure 1. (a) iron ore sample sieve 230 mesh, (b) iron ore with HCl solution, and (c) $ZnFe_2O_4$ solution.

XRD test was carried out to determine the crystal size. TEM test was performed to see the particle size of $ZnFe_2O_4$. The VSM test was undertaken to see the magnetic properties of $ZnFe_2O_4$. FTIR test is done to determine the characteristics and bonds that occur. The UV-VIS spectrophotometer test process on the ZnFe2O4 sample to determine the absorption wavelength of the synthesized $ZnFe_2O_4$.

3. Results and Discussion

3.1. Characterization of X-Ray Diffraction (XRD)

$ZnFe_2O_4$ nanoparticles obtained through the coprecipitation method were characterized using XRD. The XRD results can be seen in Figure 3. From several peaks that are known at the value of 2θ, there are 8 main peaks, 7 of which are sharp and have great intensity, this indicates that the crystallinity of $ZnFe_2O_4$ is high. The peaks are at an angle value of 2θ, which are 30.2º; 35.6º; 37.2º; 43.3º; 53.7º; 57.2º; 62.8º; 74.3º. With the fields hkl (220), (311), (222), (400), (331), (333), (440), (622). The comparison of the relative intensity data of the peaks on the XRD diagram shows conformity with the characteristics of $ZnFe_2O_4$ based on the data of the JCPDS card standard No (82-1049) with the highest peak at the Miller's index (311).

The crystal grain size of the $ZnFe_2O_4$ nanoparticles was calculated using equation *Debye Scherrer,* then the results were confirmed by the results obtained in TEM (Figure 4). By using a wavelength of 1.54060 Å, the crystal size of each $ZnFe_2O_4$ nanoparticle peaks were 3.93; 6.38; 5.75; 6.54; 4.25; 6.92; 2.54 and 2.71 nm. The average size of the $ZnFe_2O_4$ nanoparticles was in the range 4.1-15 nm, with an average particle size of 8.80 nm. The results obtained are in accordance with the size of several previous studies such as research conducted by Asmin *et al* (2015) with an average size of 8 nm also a study conducted by Vinosha *et al* (2017) which stated that the size distribution for the sample $ZnFe_2O_4$ was found to be around 8.2 nm [[6,10]. In another study, the $ZnFe_2O_4$ nanoparticles obtained in about 40 nanometers [19]. This result indicated that iron ore can be used to produce $ZnFe_2O_4$ nanoparticles. Some research on the average size of $ZnFe_2O_4$ using TEM can be viewed in Table 1.

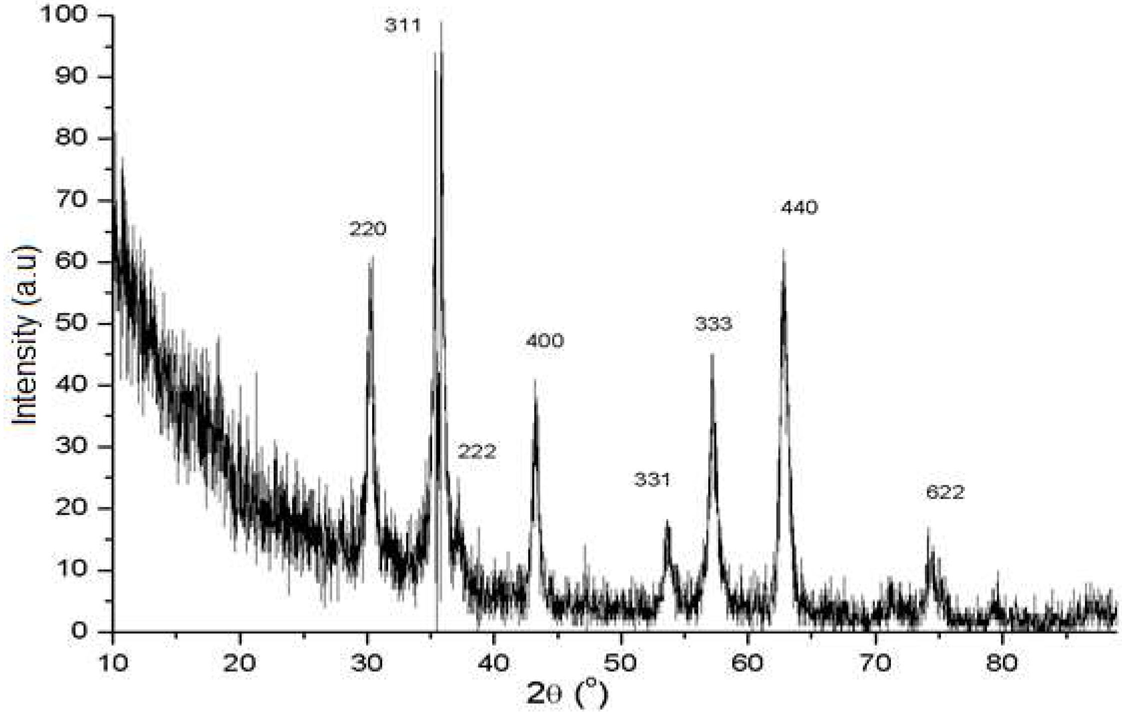

Figure 3. $ZnFe_2O_4$ diffraction patterns.

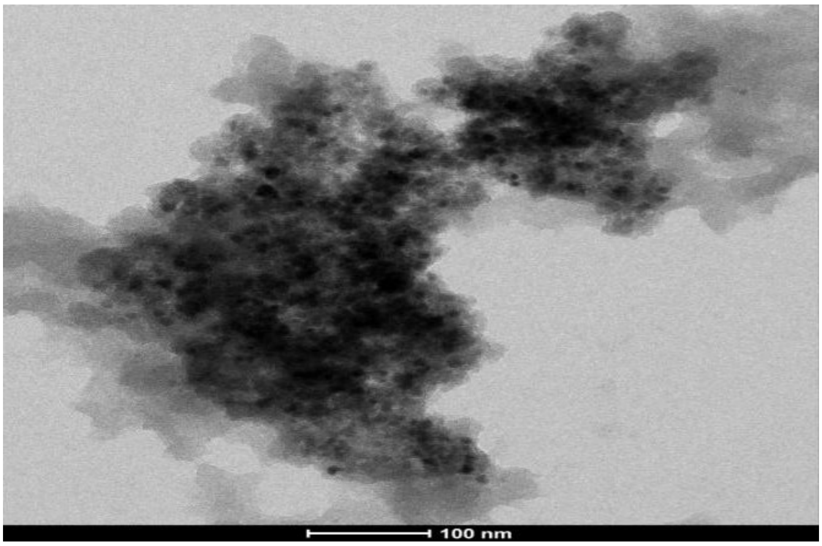

Figure 4. TEM Characterization of $ZnFe_2O_4$ nanoparticles.

Table 1. List of $ZnFe_2O_4$ mean size data from multiple references.

Methods	Measurement Mean Size	Reference
coprecipitation	8.0 nm	[6]
precipitation	8.2 nm	[10]
Hydrothermal	10.0 nm	[3]
Self-Propagating Low-Temperature Combustion	45.0 nm	[21]

3.2. *Characterization of the Vibrating Sample Magnetometer (VSM)*

Figure 5 shows the hysteresis loop and parameters of two samples of magnetic nanoparticles of Fe_3O_4 and $ZnFe_2O_4$ obtained from the characterization results using a characterization tool *Vibrating Sample Magnetometer* (VSM). From the hysteresis loop, it can be seen that $ZnFe_2O_4$ (59.81 emu/g) has a saturation magnetization value (M_s) greater than Fe_3O_4 (30.43 emu/g). This indicates that the addition of the element Zn can increase the magnetic value of this material.

Area the hysteresis curve (loop area) of $ZnFe_2O_4$ nanoparticles have a narrow loop area of 10.0 kOe.emu/g, this indicates that the material has superparamagnetic properties, because it has an invisible loop area [20]. The material can be obtained if the material has a very small size (in few nanometers), its small size causes the material to be very reactive to external magnetic fields. The hysteresis curve of $ZnFe_2O_4$ when subjected to an external magnetic field for magnetization requires very little energy with a coercivity field value (H_c) is 44.56 Oe. This shows that $ZnFe_2O_4$ is *soft magnetic*, which is the magnetic properties of a material that has value H_c a very small (<200 Oe) [20].

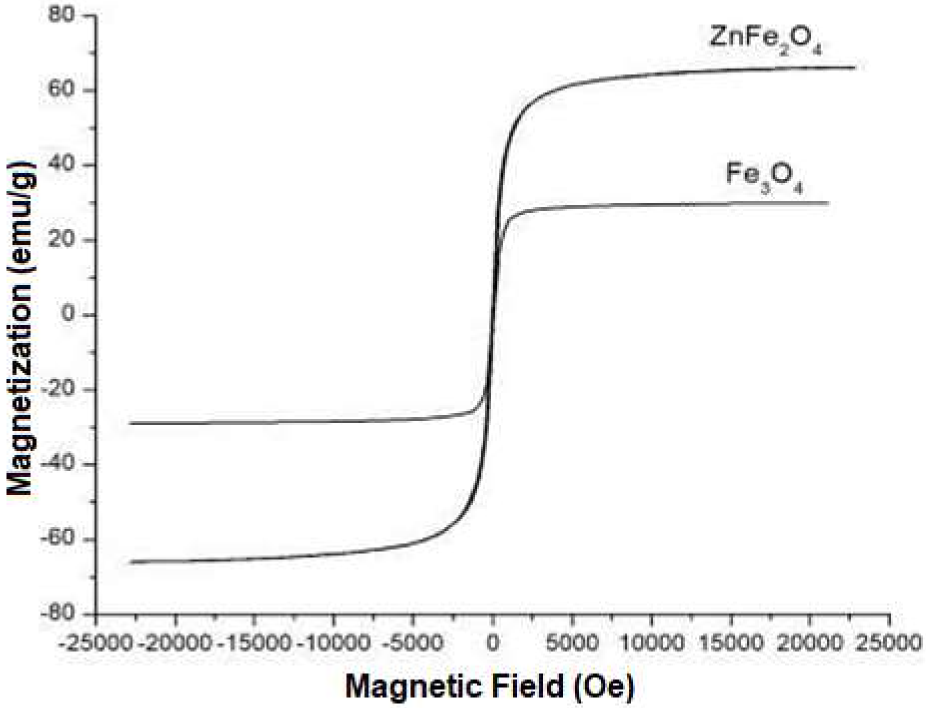

Figure 5. Hysteresis loop of Fe_3O_4 and $ZnFe_2O_4$ nanoparticles.

3.3. *Fourier Transform Infrared* (FTIR)

Characterization FTIR characterization is used to analyze the functional groups of a sample. The chemical bonds of the $ZnFe_2O_4$ nanoparticles were analyzed using the FTIR spectrum using a wavenumber between 500 - 4000 cm^{-1}. In Figure 6, it can be seen that there are absorption peaks, such as the absorption peak at the wavenumber 556.58 cm^{-1} which is the vibration mode of the metal on a tetrahedral lattice (Zn−O). In theory, the wavenumber ranges 550-750 cm^{-1} corresponds to the interaction of the metal with oxygen on a tetrahedral lattice [17,21]. The octahedral vibration mode (Fe-O) was observed at wave number 474-636 cm^{-1} [22–24]. The absorption at the widened wave number at 3318.82 cm^{-1} comes from the vibrational mode of the Hmolecule$_2$Oand the OH group, which indicates the presence of molecules H_2O on the surface of the ZnF_2O_4 nanoparticles [25,26].

In other studies, the wave absorption obtained is almost similar to this study (the absorption of wave numbers 556.58 cm^{-1}), namely in the tetrahedral lattice (Zn-O), as was done by Nurhasanah and Richardina (2018) which stated that the wave absorption was 555 cm^{-1} for vibrational modes of metals in a tetrahedral lattice (Zn − O) [7]. Subsequent research, which is also almost similar to this research, was conducted by Vinosha *et al* (2017) which states that the 547 cm^{-1} wave absorption has compatibility with metal-oxygen for the vibrational mode of metals in a tetrahedral lattice [10]. The research conducted by Asmin study *et al* (2015) is also similar to this by stating that the absorption peak group at wavenumber 555.50 cm-^{1} is a vibration mode of *stretching* Zn-Oat a *site* tetrahedral [6].

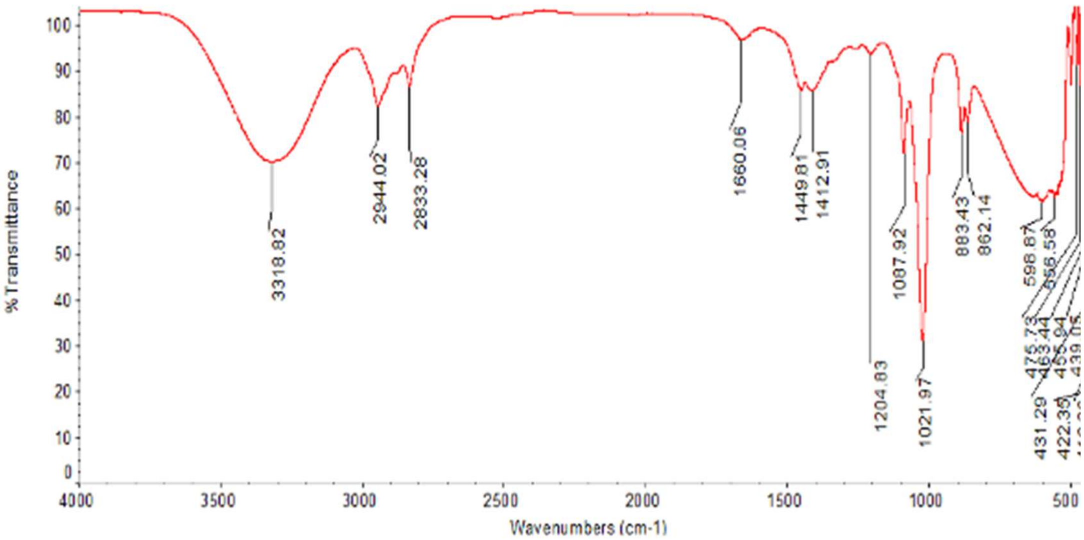

Figure 6. FTIR Spectra of $ZnFe_2O_4$ nanoparticles.

3.4. Characterization of *Spectrophotometer* UV-Vis

Testing *spectrophotometer* UV-Vis is used for the measurement of light absorption in the ultraviolet region (250-350 nm) and visible light (350-800 nm) by a compound. The optical properties of the $ZnFe_2O_4$ nanoparticles were determined based on the UV-Vis absorption spectrum, as shown in Figure 8. The absorption ability of UV light and visible light allows $ZnFe_2O_4$ nanoparticles to have photocatalytic activity with both UV and visible light which corresponds to their energy gap.

The absorbance of the sample is observed at a wavelength ranging from 200–800 nm (figure 7). Graph from the lowest point at the 800 nm wavelength, then begin to rise significantly at the 600 nm wavelength and continue to rise until it is parallel to the y-axis at 200 nm and no longer slopes about the x-axis. This shows that the $ZnFe_2O_4$ nanoparticles absorb UV light (200 nm) to visible light (600 nm).

The maximum absorption peak of $ZnFe_2O_4$ nanoparticles at wavelength of 288 nm. In a study conducted by Kumar *et al.* (2012) stated that samples of $ZnFe_2O_4$ at maximum absorption have a wavelength of 367 nm [16]. Another study conducted by Sinthiya *et al* (2014) showed two different results of absorption peaks by mixing $ZnFe_2O_4$ on PEG and CTAB, the samples tested had wavelengths of 333 and 369 nm respectively at the absorption peak [14]. The difference wavelength at the maximum absorption of this study and the two studies can occur due to differences in the purity of the materials used. This study uses nature iron ore, while the two reference studies above use commercial materials.

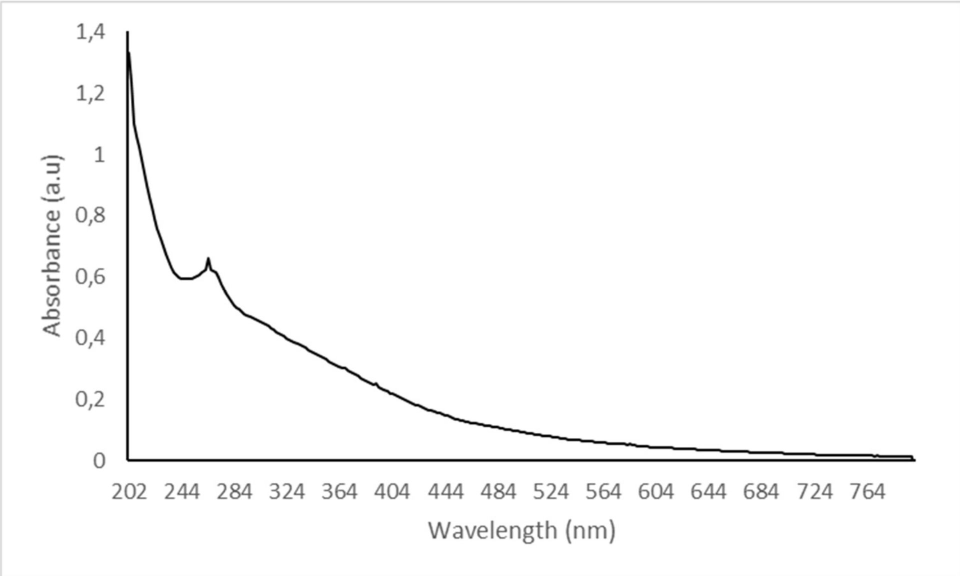

Figure 7. UV-Vis Spectrum of $ZnFe_2O_4$ nanoparticles

Based on the result of $ZnFe_2O_4$ nanoparticles, We can say that iron ore from Tanah Laut Regency can be used to produced $ZnFe_2O_4$ in range of nanometres. Furthermore, $ZnFe_2O_4$ nanoparticles can be applied to many areas like, $ZnFe_2O_4$ nanoparticles from commercial materials. In This study, we plan to use this material in biosensor, especially in biosensor glucose.

4. Conclusion

Based on the results of the research that has been undertaken, it is concluded that the average crystal size of $ZnFe_2O_4$ nanoparticle is 8.80 nm with a saturation magnetization value (M_s) of 59.81 emu/g. $ZnFe_2O_4$ is superparamagnetic with a narrow loop area of about 10 kOe.emu/g. The Zn-O functional group is observed at the wave number at 556.58 cm^{-1} and Fe-O which is observed at the wave number at 598.87 cm^{-1}. At the maximum absorption, the wavelength is 288 nm. The results showed that Zn was able to increase the saturation magnetization value of Fe_3O_4. The $ZnFe_2O_4$ nanoparticles can be applied to many field such as biomedicine, sensors, and catalysts.

5. Acknowledgement

Thank you to the Ministry of Education and Culture through the Director General of Higher Education for funding this research.

References

[1] Buschow K 2005 *Concise Encyclopedia of Magnetic and Superconducting Materials* (Elsevier Science).
[2] Meidanchi A O, Akhavan S, Khoei A, Shokri A, Hajikarimi Z and Khansari, N 2014 $ZnFe_2O_4$ Nanoparticles as Radiosensitizers in Radiotherapy of Human Prostate Cancer Cells *Material Science and Engineering* **46** 394–9.
[3] Zhang J, Song J M, Niu H L, Mao C J, Zhang S Y and Shen Y H 2015 $ZnFe_2O_4$ Nanoparticles: Synthesis, Characterization, and Enhanced Gas Sensing Property for Acetone *Sensors and Actuators, B: Chemical* **221** 55–62.
[4] Sun S, Yang X, Zhang Y, Zhang F, Ding J, Bao J and Gao C 2012 Enhanced Photocatalytic Activity of Sponge-like $ZnFe_2O_4$ Synthesized by Solution Combustion Method *Progress in Natural Science: Materials International* **22** 639 –43.

[5] Wan J, Jiang X, Li H and Chen K, 2012 Facile Synthesis of Zinc Ferrite Nanoparticles as Non-lanthanide T1 MRI Contrast Agents *Journal of Material Chemistry* **22** 13500–05.
[6] Asmin L O, Mutmainnah and Suharyadi E 2015 Effect of Particle Size on Structural and Magnetic Properties of Zinc Ferrite Nanoparticles ($ZnFe_2O_4$) *Proceedings of the XXVIII National Physics Symposium (SFN)* p 145–7.
[7] Nurhasanah I and Richardina V 2018 Photocatalysis of Zinc Ferrite Magnetic Nanoparticles Using UV Light and Visible Light the Photocatalytic of Magnetic Nanoparticles Zinc Ferrite Under UV Light and Visible Light Irradiation *Journal of Chemical Engineering and Environment* **13** 33–9.
[8] Ladole C A 2012 Preparation and Characterization of Spinel Zinc Ferrite $ZnFe_2O_4$ *International Journal of Chemical Sciences***10** 1230–4.
[9] Vazquez-olmos A R, Abatal M, Sato-berru R Y, Garcia-vazquez V, Sainz-vidal A and Quiroz A 2016 Mechanosynthesis of MFe_2O_4 (M = Co, Ni, and Zn) Magnetic Nanoparticles for Pb Removal from Aqueous Solution *Journal of Nanomaterials* **2016** 21–8.
[10] Vinosha P A, Mely L A, Jeronsia J E, Krishnan S and Das S J 2017 Synthesis and Properties of Spinel $ZnFe_2O_4$ Nanoparticles by Facile Co-Precipitation Route, *Optik - International Journal for Light and Electron Optics* **134** 99-108.
[11] Husain S, Irfansyah M, Haryanti N H, Suryajaya S, Arjo S and Maddu A 2019 Synthesis and characterization of Fe3O4 magnetic nanoparticles from iron ore. *J Phys Conf Ser 1242*.
[12] Husain S, Haryanti N H, Novalina T. Potensi Nanokomposit Fe_3O_4@C dari Bijih Besi Sebagai Pendeteksi Kadar Glukosa *Positron* **9** 44–52.
[13] Zālīte I, Heidemane G, Krūmiņa A, Rašmane D and Maiorov M 2017 $ZnFe_2O_4$ Containing Nanoparticles : Synthesis and Magnetic Properties *Material Science and Applied Chemistry* **34** 38–44.
[14] Ramamurthi K, Thangaraju M and Natesan K 2014 Synthesis of Zinc ferrite (ZnFe2O4) nanoparticles with different capping agents *International Journal of ChemTech Research* 7 1–7.
[15] Liu C, Wang B, Wang T, Liu J, Sun P, Chuai X and Lu G 2017 Enhanced gas sensing characteristics of the flower-like ZnFe2O4/ZnO microstructures *Sensors & Actuators: B. Chemical. Elsevier* **248** 902-8.
[16] Kumar G S Y, Naik H S B, Roy A S, Harish K N and Viswanath R 2013 Synthesis, Optical and Electrical Properties of $ZnFe_2O_4$ Nanocomposites *Nanomaterials and Nanotechnology* **2** 1–6.
[17] Li X, Hou Y, Zhao Q, Teng W, Hu X and Chen G 2011 Capability of novel $ZnFe_2O_4$ nanotube arrays for visible-light induced degradation of 4-chlorophenol *Chemosphere* **82** 581–6.
[18] Mufit Z and Anisa M Z 2014 *The Influence of Calcination Temperature on The Optical Properties of Hematite (α-Fe_2O_3)*, Sepuluh Nopember Institute of Technology (ITS).
[19] Swamy P M P, Basavaraja S, Lagashetty A, Srinivas-Rao N V, Nijagunappa R and Venkataraman A 2011 Synthesis and Characterization of Zinc Ferrite Nanoparticles Obtained by Self-Propagating Low-Temperature Combustion Method *Bulletin of Materials Science* **34** 1325–30.
[20] Pauzan M, Kato T, Iwata S and Suharyadi E 2013 *The Effect of Grain Size and Crystal Structure on Magnetic Properties in Magnetite Nanoparticles (Fe 3 O 4), Proceedings of the XXVII HFI Scientific Meeting* p. 24-8.
[21] Li W, Wu X, Chen J, Gong Y, Han N and Chen Y 2017 Abnormal npn type conductivity transition of hollow ZnO/$ZnFe_2O_4$ nanostructures during gas sensing process: The role of ZnO-ZnFe2O4 hetero-interface *Sensors & Actuators: B. Chemical* **253** 144-155.
[22] Cornel R M and Schwertmann U 1996 *The Iron Oxides: Structures, Properties, Reactions, Occurences and Uses*.
[23] Lakay E M 2009 *Superparamagnetic Iron-Oxide Based Nanoparticles for the Separation and Recovery of Precious Metals from Solution* (University of Stellenbosch).
[24] Ihsani S I, Ekaputra P A, Asri L A T W and Purwasasmita B S 2015 Encapturization of Fe_3O_4

Superparamagnetic Nanoparticles Using Mangosteen Impregrated Chitosan and Alginate and Morphological Modification Using Chitosan and Tapioca *Research and Development on Nanotechnology in Indonesia* **2** 91–8.
[25] Dachriyanus P D 2004 *Structural Analysis of Organic Compounds by Spectroscopy* (LPTIK Andalas University).
[26] Jin Z, Dong Y, Dong N, Yang Z, Wang Q, Lei Z and Su B 2017 One-step synthesis of magnetic nanocomposite Fe_3O_4/C based on the waste chicken feathers by a green solvothermal method *Materials Letters* **186** 322–5.